Original Article

JCBFM

Journal of Cerebral Blood Flow & Metabolism
2021, Vol. 41(10) 2743–2755

DOI: 10.1177/0271678X211012153
journals.sagepub.com/home/jcbfm
SAGE

Impaired cerebral vascular and metabolic responses to parametric N-back tasks in subjective cognitive decline

Yaoyu Zhang[1,2,*], Wenying Du[3,*], Yayan Yin[4], Huanjie Li[5], Zhaowei Liu[6], Yang Yang[2], Ying Han[3,7,8,9] and Jia-Hong Gao[2,10,11]

Abstract

Previous studies reported abnormally increased and/or decreased blood oxygen level-dependent (BOLD) activations during functional tasks in subjective cognitive decline (SCD). The neurophysiological basis underlying these functional aberrations remains debated. This study aims to investigate vascular and metabolic responses and their dependence on cognitive processing loads during functional tasks in SCD. Twenty-one SCD and 18 control subjects performed parametric N-back working-memory tasks during MRI scans. Task-evoked percentage changes (denoted as δ) in cerebral blood volume (δCBV), cerebral blood flow (δCBF), BOLD signal (δBOLD) and cerebral metabolic rate of oxygen ($\delta CMRO_2$) were evaluated. In the frontal lobe, trends of decreased δCBV, δCBF and $\delta CMRO_2$ and increased δBOLD were observed in SCD compared with control subjects under lower loads, and these trends increased to significant differences under the 3-back load. δCBF was significantly correlated with $\delta CMRO_2$ in controls, but not in SCD subjects. As N-back loads increased, the differences between SCD and control subjects in δCBF and $\delta CMRO_2$ tended to enlarge. In the parietal lobe, no significant between-group difference was observed. Our findings suggested that impaired vascular and metabolic responses to functional tasks occurred in the frontal lobe of SCD, which contributed to unusual BOLD hyperactivation and was modulated by cognitive processing loads.

Keywords

Subjective cognitive decline (SCD), cerebral blood volume (CBV), cerebral blood flow (CBF), blood oxygen level-dependent (BOLD), cerebral metabolic rate of oxygen ($CMRO_2$)

Received 15 September 2020; Revised 19 February 2021; Accepted 1 April 2021

[1]Institute for Medical Imaging Technology, School of Biomedical Engineering, Shanghai Jiao Tong University, Shanghai, China
[2]Center for MRI Research, Academy for Advanced Interdisciplinary Studies, Peking University, Beijing, China
[3]Department of Neurology, Xuanwu Hospital of Capital Medical University, Beijing, China
[4]Department of Radiology, Xuanwu Hospital of Capital Medical University, Beijing, China
[5]School of Biomedical Engineering, Dalian University of Technology, Dalian, China
[6]Center for Excellence in Brain Science and Intelligence Technology (Institute of Neuroscience), Chinese Academy of Sciences, Shanghai, China
[7]Biomedical Engineering Institute, Hainan University, Haikou, China
[8]Center of Alzheimer's Disease, Beijing Institute for Brain Disorders, Beijing, China
[9]National Clinical Research Center for Geriatric Disorders, Beijing, China
[10]Beijing City Key Lab for Medical Physics and Engineering, Institute of Heavy Ion Physics, School of Physics, Peking University, Beijing, China
[11]McGovern Institute for Brain Research, Peking University, Beijing, China

*These authors contributed equally to this paper.

Corresponding authors:
Jia-Hong Gao, Center for MRI Research, Peking University, Beijing 100871, China.
Email: jgao@pku.edu.cn

Ying Han, Department of Neurology, Xuanwu Hospital of Capital Medical University, Beijing 100053, China.
Email: hanying@xwh.ccmu.edu.cn

Introduction

Subjective cognitive decline (SCD) is characterized by a self-perceived continuous worsening of cognitive functions with no objective impairment in cognition.[1,2] SCD has a high incidence in the elderly population,[3,4] increases the risk of Alzheimer's dementia (AD)[5] and may be the first cognitive manifestation of AD.[2] Investigations of the brain mechanisms of SCD have immediate significance to the early detection and prognosis of AD.

Functional brain aberrations exist in SCD[6] and occur early in the course of AD.[7] During cognitive tasks, various laboratories observed abnormally elevated and/or lowered blood oxygen level-dependent (BOLD) activation in the prefrontal cortex and other brain regions in SCD compared with control subjects.[8–13] Interpretations of how SCD modulates functional brain activity, therefore, remain debatable. One leading theory favors compensatory strategies, where increased functional activity arises from additional neuronal recruitment to maintain cognitive integrity.[8–11,14,15] An alternative view suggests continuous mild neural impairments. In this regard, compromised functional activity can be associated with vascular dysfunction,[16] hypometabolism[17] and other neuronal deficiencies.[13,18] The above theories were primarily tested in SCD using BOLD functional magnetic resonance imaging (fMRI).[8–13] Although the BOLD signal has merits, including robustness, ease of use, and relatively high spatial and temporal resolution, it reflects a mixed effect of changes in cerebral blood volume (CBV), cerebral blood flow (CBF) and cerebral metabolic rate of oxygen ($CMRO_2$).[19] This prompts us to look beyond the BOLD signal to gain insights into the neurophysiological basis of functional brain aberrations in SCD. We hypothesized that, compared with control subjects, those with SCD would have elevated vascular and metabolic changes during cognitive tasks if the compensatory mechanism was triggered. Otherwise, continuous neural impairment might occur, which could limit the vascular and metabolic responses of SCD subjects. Unfortunately, a study clarifying vascular and metabolic behavior during functional brain activation in SCD has not been reported.

Moreover, the functional brain aberrations in SCD might be dependent on cognitive processing loads. In behavioral studies, people with SCD performed normally on standardized cognitive tests but fell behind on complex cognitive tasks.[13,20–22] In neuroimaging studies, BOLD activation evoked by the N-back task was comparable between SCD and control groups under lower loads (1∼2 back) but significantly increased in SCD under higher loads (2∼3 back).[8,11] These findings suggested the possibility of a load-dependent approach to SCD assessment. However, the association between cognitive task loads and functional brain aberrations in SCD has not been explored from vascular and metabolic perspectives. The N-back paradigm is suitable for addressing this issue because it allows manipulation of working memory loads and evokes load-dependent functional brain activation.

In this study, we applied well-established multimodal MRI techniques and parametric N-back working memory tasks to investigate (a) the underlying vascular and metabolic mechanisms of functional brain aberrations and (b) their associations with working memory loads in SCD. Age- and education-matched SCD and control subjects performed 0-, 1-, 2- and 3-back tasks in an MRI scanner. Cerebrovascular regulation was assessed with an MRI pulse sequence that simultaneously acquired task-evoked changes in CBV, CBF and the BOLD signal.[23–30] Task-evoked changes in $CMRO_2$ were evaluated with a modified BOLD calibration model.[25–27] The results of this study may pave the way to understanding the neurological mechanism underlying functional brain aberrations in SCD, which would provide critical information for the early detection and prognosis of AD.

Materials and methods

Subjects

Twenty-two SCD subjects and 20 age- and education-matched control subjects aged 60-79 years were recruited from the community via advertisements between June 2018 and October 2019. This study was approved by the Ethics Committee of Peking University (approval number: 2016-03-08), in accordance with the Helsinki Declaration of 1975 (and as revised in 1983). Written informed consent was obtained from each subject. All subjects completed systematic neuropsychological assessments, physical examinations and MRI scans. The subjects abstained from caffeine and alcohol for at least 12 hours prior to the MRI scans.

The inclusion criteria for the SCD group were in accordance with the research criteria proposed by Jessen and colleagues,[2] namely, elderly adults with normal cognitive performance after age, gender and education adjustment who reported the presence of persistent self-perceived cognitive decline, unrelated to acute events, compared with their previous normal cognitive status.[2] To include subjects at high risk for cognitive decline, we explicitly sought out subjects who had complaints and concerns about memory decline, but not declines in other cognitive functions, within the past five years.[1] The inclusion criteria for the

control group called for cognitively normal elderly adults with no complaints.

The exclusion criteria for all subjects included mild cognitive impairment (MCI) or dementia, which was diagnosed based on the Jak and Bondi criteria[31] or the Diagnostic and Statistical Manual of Mental Disorders, fifth edition (DSM-5),[32] respectively; major psychiatric diseases, such as severe depression and anxiety; neurological conditions that may affect brain structure or function (e.g., stroke, brain tumors, epilepsy, or Parkinson's disease); systemic diseases that may lead to cognitive decline, such as thyroid dysfunction, severe anemia, syphilis or HIV; cognitive impairments caused by traumatic brain injury; uncontrolled diabetes or hypertension; abuse of tobacco, alcohol or drugs; inability to complete the protocol; and contraindications for MRI.

One SCD subject and two control subjects were excluded due to excessive head motion during MRI scans. The results of this study were based on 21 SCD (13 females) and 18 control subjects (10 females).

Clinical and cognitive assessments

All subjects completed a systematic inquiry into their basic information and medical history as well as a battery of neuropsychological tests, which included the following: the Subjective Cognitive Decline Interview (SCD-I) and 9-item Subjective Cognitive Decline Questionnaire (SCD-Q9) to evaluate the details of self-reported complaints and the severity level of SCD; the Hamilton Anxiety Scale (HAMA)/ Hamilton Depression Scale (HAMD) and Geriatric Depression Scale (GDS) to evaluate emotions and moods; the Auditory Verbal Learning Test (AVLT) with long delayed recall and recognition to evaluate the cognitive domain of memory; the Shape Trail Test-A/B (STT-A/B) to evaluate the cognitive domains of speed and executive function; the Boston Naming Test (BNT) and Animal Fluency Test (AFT) to evaluate the cognitive domain of language; the Functional Activities Questionnaire (FAQ) to evaluate activities of daily living; and the Montreal Cognitive Assessment-Basic (MoCA-B) to evaluate global cognitive function. Details on the protocols and cutoffs of the aforementioned neuropsychological assessments have been previously published.[33] The inquiries were conducted by a professional neurologist, and the diagnoses were confirmed by two experienced neurologists.

Experimental procedures

All subjects were briefly trained for familiarization with the experimental procedures before the MRI scans.

N-back task. The block-designed N-back task was composed using E-Prime software (Psychology Software Tools, Pittsburgh, PA, USA). Each block consisted of a cue (2 s) and a series of 15 one-digit numbers (30 s). Each number was displayed for 0.5 s, followed by a "+" for 1.5 s. During a baseline (0-back) block, subjects were instructed to press a button as soon as the number "3" was displayed. During an active (1-, 2- or 3-back) block, subjects were instructed to press the button when the current number matched the number that preceded it by 1, 2 or 3 places, respectively.

Each run of the N-back task lasted 148 s, which consisted of a 12-s dummy scan, a baseline block followed by the three active blocks in a pseudorandom order, and an 8-s resting session. Each subject completed six runs of the N-back task to permit a sequentially balanced design of the three active blocks. All subjects' responses were recorded. The hit rate, false alarm rate, dprime (i.e., difference between the z-transforms of the hit rate and false alarm rate) and reaction time were used to evaluate subjects' N-back task performance.

CO_2 challenge. Following the N-back task, a CO_2 challenge was adopted from a previous study[24] to allow the evaluation of the N-back task-induced $CMRO_2$ changes using the modified BOLD calibration model.[25–27] Subjects were supplied with medical air (21% O_2 and 79% N_2) for the first 132 s and a hypercapnic gas mixture (5% CO_2, 21% O_2 and 74% N_2) for the remaining 180 s via a laboratory-built gas supply system.[24] During the CO_2 challenge, the arterial oxygen saturation (%SPO_2) and pulse rate of 15 subjects (7 control and 8 SCD subjects) were measured with a digital pulse oximeter (Model 7500 FO, Nonin Plymouth, USA). These measurements were not significantly different between the two groups (%SPO_2 – normocapnia (controls vs. SCD, mean ± standard deviation (SD)): 95.62 ± 1.72 vs. 96.61 ± 1.51, $p = 0.26$, hypercapnia: 96.17 ± 2.35 vs. 97.54 ± 1.11, $p = 0.16$; pulse rate – normocapnia: 82.94 ± 6.33 vs. 78.09 ± 7.06, $p = 0.19$, hypercapnia: 80.80 ± 7.51 vs. 76.04 ± 6.25, $p = 0.20$). Other physiological parameters were not monitored in this study, but nonetheless merit attention and will be studied in our future work with larger samples.

MRI scanning protocol

All imaging data were collected on a 3.0 T MRI system (Discovery MR750, GE Healthcare, Milwaukee, WI, USA) equipped with an 8-channel head coil. For fMRI acquisition, the common parameters were field of view (FOV) = 260×260 mm^2, matrix = 64×64, slice thickness = 6 mm and time of repetition (TR) = 2 s. All subjects sequentially underwent a functional localizing run, the N-back task and the CO_2 challenge. The

functional localizing run consisted of a dummy scan and six blocks alternating between 0-back and 2-back tasks (204 s). During the functional localizing run, whole-brain BOLD signals were acquired using a T_2*-weighted gradient-echo echo-planar imaging sequence with the following parameters: time of echo (TE) = 30 ms, flip angle = 90°, 10 slices. Immediately after the functional localizing run, the built-in fMRI analysis platform on the MRI system was used to identify an oblique slice through the 2-back activation regions in both the frontal and parietal lobes for each subject as the targeted imaging slice for the rest of the MRI scan. During the subsequent N-back task and the CO_2 challenge, CBV-, CBF- and BOLD-weighted signals were acquired in the target slice using a simultaneous vascular space occupancy (VASO), arterial spin label (ASL) and BOLD acquisition sequence[23,24] with the following parameters: TE = 9.4/11.6/28.1 ms for VASO/ASL/BOLD signals, inversion slab = 102 mm. The blood nulling time (TI_1) for the VASO signal was individually determined with an inversion recovery sequence by searching for the lowest signal intensity in the sagittal sinus.[23,24] TI_2 for the ASL signal was 1200 ms.[24,26] Finally, a structural image of the same position was acquired using a T1-weighted fluid-attenuated inversion recovery sequence as previously described.[24]

MRI data processing

All functional images were analyzed using AFNI software (AFNI_19.1.00, https://afni.nimh.nih.gov/) and customized MATLAB (version 9.1.0, MathWorks, Natick, MA, USA) scripts. Images obtained during the dummy scans were discarded. In order to account for motion-related effects, outliers in each time series were detected using the 3dToutCount command and later inputted as a nuisance regressor in the general linear model (GLM) analysis. The VASO/ASL/BOLD images were obtained by surround averaging/subtraction/averaging of the adjacent label and control images acquired during the first/second/third echo of the simultaneous acquisition sequence, respectively.[24] Spatial smoothing was performed with an 8-mm Gaussian kernel. Images during all six runs of the N-back task were scaled to a mean of 100 and concatenated. GLM analyses were performed to identify voxels that were positively activated by the 1-, 2- and 3-back tasks with respect to the 0-back task and by hypercapnia with respect to normocapnia. The criterion for statistical significance was $p < 0.05$. For each task, the region of interest (ROI) was selected as the voxels that were activated for all of the VASO, ASL and BOLD signals. ROIs in the frontal and parietal lobes were distinguished by the central sulcus.

Herein, we defined δ as the percentage change in a signal. For example, $\delta BOLD = BOLD/BOLD_0 - 1$, where BOLD and $BOLD_0$ represent the average BOLD signals measured in the activated and baseline states, respectively. Within each ROI, voxelwise δVASO, δASL and δBOLD were calculated for the N-back task and the CO_2 challenge. δCBV was converted from δVASO as previously described,[24,26] and $\delta CBF = \delta ASL$.

A modified BOLD calibration model[24,26,27] was adopted for the calculation of $\delta CMRO_2$ evoked by the N-back task:

$$\delta BOLD = M\left[1-(\delta CBV+1)\left(\frac{\delta CMRO_2+1}{\delta CBF+1}\right)^{\beta}\right] \quad (1)$$

In equation (1), β is a constant characterizing the relationship between the BOLD signal and the magnetic susceptibility difference between blood and tissue. $\beta e = 1.5$, simulated with 2% capillary and 2% venule volume fractions,[34] was selected for this study.[24,26,27] A lower $\beta = 0.8 \sim 1$ has also been suggested[35–37] and may have minor effects on the results.[24,34,36] For each subject, M, the BOLD calibration parameter, can be calculated by solving equation (1) with the δCBV, δCBF and δBOLD measured during the CO_2 challenge under the assumption that the $CMRO_2$ does not change between normocapnic and hypercapnic conditions (i.e., $\delta CMRO_2 = 0$). Next, M and the δCBV, δCBF and δBOLD obtained during the N-back task were entered into equation (1) to calculate the $\delta CMRO_2$ evoked by the N-back task. Finally, these measurements were averaged within each ROI for each subject.

Statistical analysis

The statistical analysis was performed using SPSS software (version 26, IBM Corporation, Somers, NY, USA). Data normality was tested using the Kolmogorov-Smirnov test. Demographic, clinical, cognitive and neuroimaging parameters were compared between the SCD and control groups. Continuous variables were analyzed via one-way analysis of covariance (ANVOCA) and its non-parametric equivalent as appropriate, while categorical variables were analyzed via chi-square test. Since the neuroimaging parameters in the parietal lobe did not show significant differences between the two groups (see details in the Results section), they were not further investigated. In the frontal lobe, partial correlations were evaluated among the neuroimaging parameters as well as between the neuroimaging parameters and the MoCA-B scores. Throughout the statistical analysis, age, gender and education were considered covariates, and $p < 0.05$

after false discovery rate (FDR) correction was used as the threshold for statistical significance.

Results

Behavioral results

The SCD and control groups were matched with respect to age (mean ± SD: 65.86 ± 4.03 vs. 68.83 ± 5.93, $p = 0.07$) and education (13.38 ± 2.64 vs. 13.50 ± 3.17, $p = 0.90$). Their clinical and cognitive results are displayed in Table 1. The SCD group had higher SCD-Q9, HAMD and HAMA scores than the control group. Otherwise, the two groups performed comparably during the objective cognitive assessments. In addition, their N-back task performance was equivalent ($p > 0.26$ for all hit rates, false alarm rates, dprimes and reaction times, Figure 1).

Neuroimaging results

Figure 2 provides an overview of the anatomical (Figure 2(a)) and functional (Figure 2(b) and (d)) information of a representative SCD subject generated by the MRI procedures. Note that all SCD and control subjects had task-induced activation in the frontal and parietal ROIs (i.e., voxels activated for all δCBV, δCBF and δBOLD), with no significant difference in the numbers of activated voxels between the two groups (frontal ROIs – CO_2 challenge (SCD vs. controls, mean ± SD): 30.71 ± 19.11 vs. 32.88 ± 20.81, $p = 0.71$, 1-back: 13.19 ± 16.36 vs. 11.78 ± 12.31, $p = 0.66$, 2-back: 26.81 ± 24.59 vs. 26.67 ± 24.25, $p = 0.65$, 3-back: 27.33 ± 29.87 vs. 24.83 ± 24.20, $p = 0.87$; parietal ROIs – CO_2 challenge: 63.00 ± 33.56 vs. 67.29 ± 47.39, $p = 0.75$, 1-back: 35.10 ± 33.47 vs. 27.61 ± 26.04, $p = 0.31$, 2-back: 62.81 ± 47.04 vs. 58.94 ± 47.59, $p = 0.96$, 3-back: 62.43 ± 45.76 vs. 55.78 ± 54.01, $p = 0.78$). As displayed in Figure 2(c), the 1-back task evoked lesser functional activations, in terms of both area and intensity, than the 2- and 3-back tasks. The hypercapnia measurements led to the M map, which was used to calculate $\delta CMRO_2$ within the ROIs for each task (Figure 2(d)). The mean M values were not significantly different between the two groups (frontal ROI (SCD vs. control, mean ± SD) 0.060 ± 0.029 vs. 0.049 ± 0.026, $p = 0.26$; parietal ROI 0.069 ± 0.038 vs. 0.058 ± 0.019, $p = 0.33$).

The quantitative group averages of δCBV, δCBF, δBOLD and $\delta CMRO_2$ evoked by the N-back task are shown in Figure 3. In the frontal lobe, the SCD group tended to have lower δCBV, δCBF and $\delta CMRO_2$ as well as higher δBOLD than the control group. Specifically, all 3-back neuroimaging parameters, 1-back δCBV and 2-back δBOLD were significantly different ($p < 0.05$ after FDR correction for all occasions) between the two groups. Notably, the between-group differences tended to increase with N-back loads in δCBF and $\delta CMRO_2$, but such trends were not clearly evident in δCBV or δBOLD. In the parietal lobe, none of the task-evoked functional changes were significantly different between the two groups.

For all the 1-, 2- and 3-back tasks, δCBF and $\delta CMRO_2$ in the frontal lobe were strongly correlated ($p < 0.01$ after FDR correction for all occasions, Figure 4) in the control group but uncorrelated in the SCD group. Additionally, δCBF was positively correlated with the MoCA-B score ($p < 0.05$ after FDR correction, Figure 5(a)) in both groups for nearly all N-back cases (the only exception being the 1-back task in the

Table 1. Clinical and cognitive results.

Neuropsychological test	SCD (N = 21)	Control (N = 18)	P value
MoCA-B	25.62 ± 2.31	25.44 ± 1.82	0.78
SCD-Q9	5.00 ± 1.80	2.33 ± 1.49	<0.01
HAMD	4.10 ± 3.79	1.83 ± 1.79	0.04
HAMA	4.62 ± 3.87	1.72 ± 2.32	<0.01
AVLT: long delayed recall	6.24 ± 1.64	6.33 ± 1.37	0.83
AVLT: recognition	21.90 ± 1.58	21.33 ± 1.46	0.30
STT-A	63.10 ± 14.88	61.33 ± 15.40	0.38
STT-B	140.81 ± 42.22	137.11 ± 38.89	0.50
AFT	18.90 ± 5.22	18.67 ± 5.09	0.91
BNT	25.38 ± 2.36	24.06 ± 3.23	0.18
GDS	2.33 ± 1.80	1.39 ± 1.42	0.12
FAQ	0.19 ± 0.68	0.06 ± 0.24	0.46

SCD: subjective cognitive decline; MoCA-B: Montreal Cognitive Assessment-Basic; SCD-Q9: 9-item Subjective Cognitive Decline Questionnaire; HAMD: Hamilton Depression Scale; HAMA: Hamilton Anxiety Scale; AVLT: Auditory Verbal Learning Test; STT: Shape Trail Test; AFT: Animal Fluency Test; BNT: Boston Naming Test; GDS: Geriatric Depression Scale; FAQ: Functional Activities Questionnaire.
Note: Values are mean ± SD. P values were obtained by performing analyses of covariance with age, gender and education as covariates.

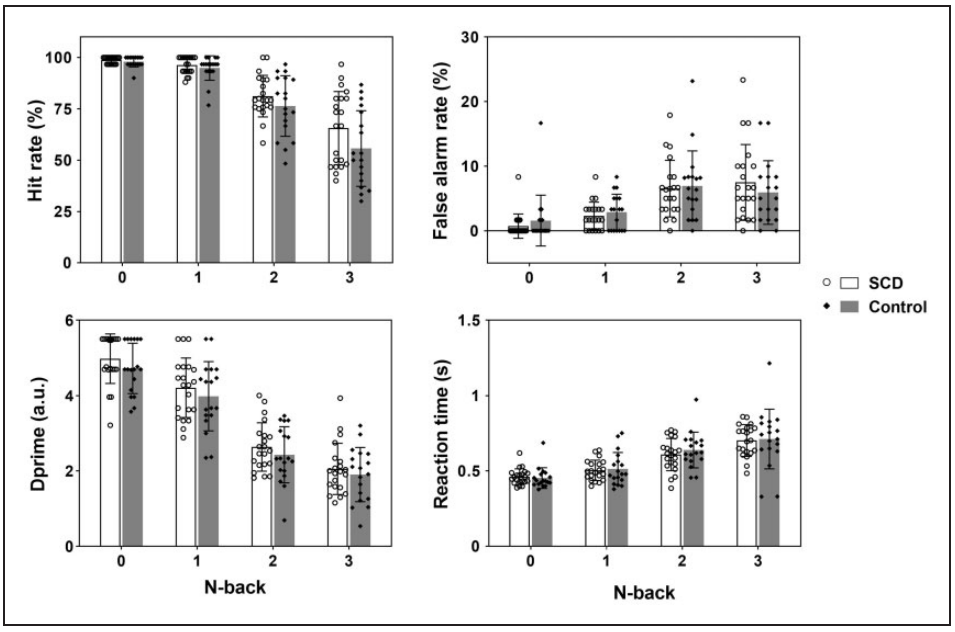

Figure 1. The average hit rates, false alarm rates, dprimes, and reaction times (mean ± SD with exact data points) exhibited no significant differences ($p > 0.26$ for all occasions) between the SCD and control groups during the 0-, 1-, 2- or 3-back task.

control group). In contrast, $\delta CMRO_2$ was positively correlated with the MoCA-B score only in the control group during the 2- and 3-back tasks ($p < 0.05$ after FDR correction, Figure 5(b)) and uncorrelated in the SCD group.

Discussion

In this study, we investigated task-evoked cerebral vascular and metabolic responses and their dependence on cognitive processing loads in SCD. To achieve this goal, we implemented a well-established simultaneous MRI acquisition technique[23–30] to measure task-evoked δCBV, δCBF and $\delta BOLD$ in a time-efficient manner. Additionally, a sophisticated BOLD calibration model[24–27,34,38] was adopted to evaluate task-evoked $\delta CMRO_2$. These neuroimaging parameters were measured and evaluated during a parametric N-back working memory task performed by age- and education-matched SCD and control cohorts.

Our main finding was that decreased δCBV, δCBF and $\delta CMRO_2$ and increased $\delta BOLD$ concurrently occurred in SCD compared with control subjects. Previous fMRI studies mostly used the BOLD signal to investigate cognitive functions in SCD.[8–13] Some reported increased BOLD activation and explained their observations as a compensatory strategy to maintain cognitive function,[8–11] whereas others reported lower BOLD activation and attributed their observations to neural deficiency.[12,13] Similarly, a mixture of increased and decreased BOLD activation during working memory tasks has been reported in amnestic MCI (aMCI) and/or AD patients compared to control subjects.[39–42] Since the BOLD signal reflects a mixed effect of many physiological parameters, including CBV, CBF and $CMRO_2$, changes in this signal could be induced by vascular factors in addition to neuronal activation. In this study, our observation of increased BOLD activation in SCD could not be adequately explained by a compensatory mechanism with the presence of compromised vascular and metabolic responses. Instead, we propose that cognitive-related vascular and metabolic impairments occurred in SCD subjects.

Previous studies have stressed the nonnegligible role of vascular dysregulation during the early stage of AD.[43–45] In the resting state, global and regional CBF was reported to decrease over the course of neurodegeneration by multiple studies using various techniques.[46] Such decreased resting CBF was associated with impaired cognitive functions in SCD[16,47] and was proposed to predict cognitive decline in elderly individuals.[48] In this study, resting CBF was not directly measured but was theoretically proportional to the ASL data via the following equation[29,49,50]:

$$CBF = \frac{\lambda ASL}{2\alpha M_0 \tau e^{-(TI_2/T_{1a})}} \quad (2)$$

where ASL represents the label/control-subtracted ASL images; λ is the blood-tissue partition coefficient; α and τ are the labeling efficiency and duration,

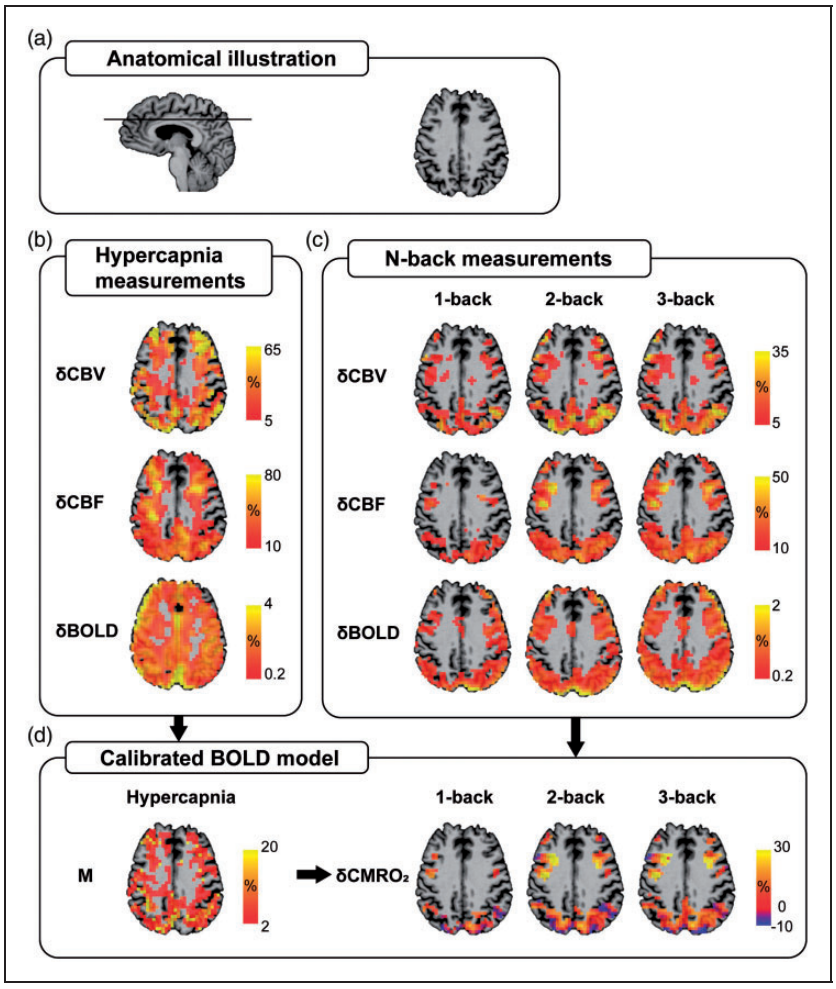

Figure 2. Maps of a representative subject (Female, 66 years old) from the SCD group are presented for illustrative purposes. (a) Anatomical information on the imaging slice. Voxel-based δCBV, δCBF and δBOLD evoked by (b) the CO_2 challenge and (c) the 1-, 2- and 3-back tasks with respect to the 0-back task were measured using the simultaneous MRI acquisition technique. The activated voxels were identified using GLM analysis, with $p < 0.05$ considered statistically significant. (d) The calibrated BOLD model was used to obtain the M value resulting from the CO_2 challenge, which, in turn, was used to calculate $\delta CMRO_2$ during the 1-, 2- and 3-back tasks. The ROI of each task was determined by finding the commonly activated voxels across all CBV, CBF and BOLD measurements. All functional maps were overlaid on the subject's structural image.

respectively; M_0 is the equilibrium brain tissue magnetization; and T_{1a} is the blood T_1. Based on a bold assumption that λ, M_0 and T_{1a} were not affected by SCD, we compared the ASL data obtained during the baseline period of the CO_2 challenge and found no significant difference between the two groups (ASL signals (control vs. SCD, mean $\pm$ SD): 53.07 ± 12.89 vs. 53.69 ± 11.87, $p = 0.31$). On the other hand, few studies have examined task-state CBF responses in SCD or AD. Studies of aMCI patients reported decreased regional CBF responses to memory-encoding tasks compared to control subjects.[51,52] Consistent with the aMCI findings, the present study reported a reduced task-evoked δCBF in the frontal lobe of the SCD group. Based on the previous findings of a declined (or unchanged) resting CBF in the SCD group, the reduced δCBF observed in this study could imply a reduced absolute change in CBF. According to Lu et al.,[53] the VASO-based δCBV primarily reflects the absolute CBV changes under the approximation that baseline CBV is relatively small in the brain parenchyma. We reported decreased N-back task-evoked δCBV in the frontal lobe of the SCD group, which was also consistent with the reduced δCBF observation if one considers their close relationship.[54] Together, our findings of compromised δCBV and δCBF further demonstrated impaired cerebrovascular regulation during comprehensive tasks in SCD.

Reduced $\delta CMRO_2$ was also observed in the frontal lobe of the SCD group during the N-back task. To the best of our knowledge, no reported fMRI study has investigated task-evoked $CMRO_2$ changes in SCD or

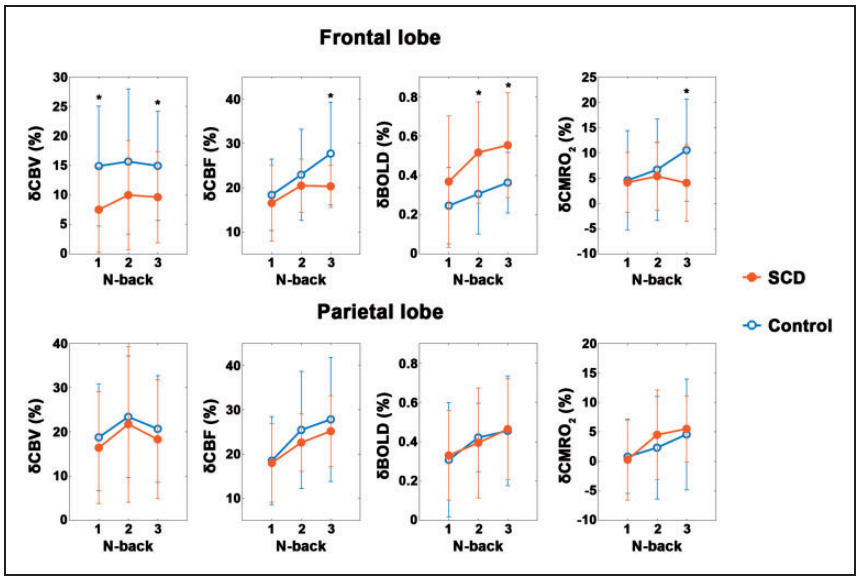

Figure 3. The average δCBV, δCBF, δBOLD and $\delta CMRO_2$ (mean $\pm$ SD) evoked by the 1-, 2- and 3-back tasks with respect to the 0-back task in the frontal and parietal lobes of the SCD and control groups. GLM analyses were applied to compare the percentage changes between the two groups with age, gender and education as covariates. * denotes $p < 0.05$ after FDR correction.

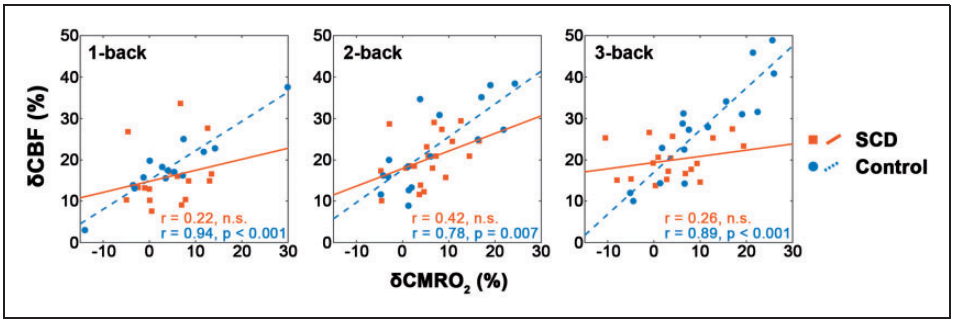

Figure 4. During 1-, 2- and 3-back tasks, significant positive correlations were observed in the frontal lobe between δCBF and $\delta CMRO_2$ in the control group but not in the SCD group. These FDR-corrected partial correlations were performed with age, gender and education as covariates.

AD. Xu et al. showed no difference in the mean $CMRO_2$ changes during a memory-encoding task but a significantly decreased activation index (i.e., mean $CMRO_2$ changes multiplied by the ratio of activated to total voxels in the hippocampus) in aMCI patients compared to control subjects.[55] Using the functional near-infrared spectroscopy technique, a majority of the studies reported hypoactivation in cerebral oxygenation, which can be related to relative $CMRO_2$ and CBF changes by fitting into a biophysical model,[56,57] in the frontal/parietal cortex of aMCI and AD patients during working memory[58–60] and other cognitive tasks.[61] In the resting state, reduced[17,62] or unchanged[63] levels of glucose metabolism were observed in SCD compared with control subjects. As the resting cerebral metabolic rates of glucose and oxygen are closely coupled,[64] the SCD group likely had a reduced or unchanged resting $CMRO_2$ and a reduced absolute increase in $CMRO_2$ during the N-back task. Additionally, δCBF was disassociated from $\delta CMRO_2$ in SCD (Figure 4), which was also reported in aMCI patients[65] and suggested impaired neurovascular coupling. Moreover, the correlation between $\delta CMRO_2$ and the MoCA-B score observed in controls appeared to diminish in SCD subjects (Figure 5(b)). Together, these alterations in metabolism could be a manifestation of impaired neuronal[66] or blood-brain barrier[43] integrity.

Evaluation of $\delta CMRO_2$ with the modified BOLD calibration model relies on a crucial assumption that the CO_2 challenge is an isometabolic procedure.[34] In practice, both unchanged and decreased $CMRO_2$ with mild hypercapnia have been reported in human studies.[67] If $CMRO_2$ had decreased during the CO_2

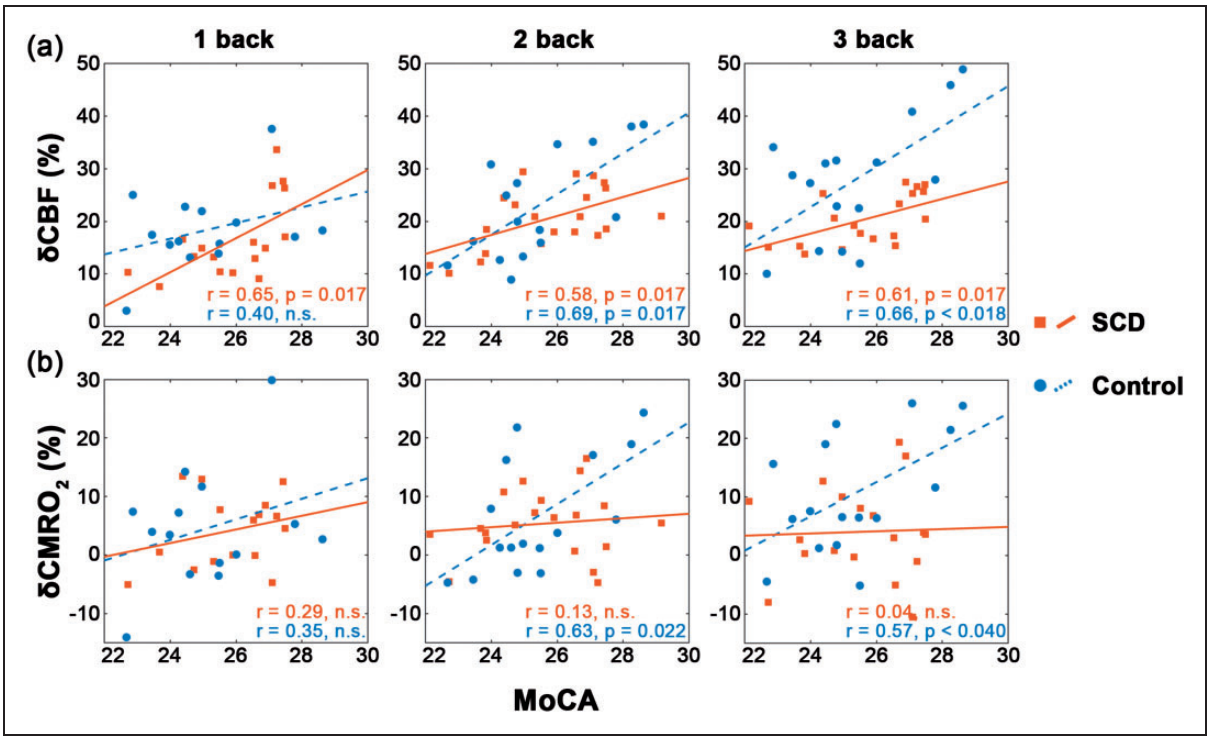

Figure 5. In the frontal lobe, (a) δCBF was positively correlated with the MoCA-B score in the SCD group during all the 1-, 2- and 3-back tasks and in the control group during the 2- and 3-back tasks; (b) $\delta CMRO_2$ was positively correlated with the MoCA-B score in the control group during the 2- and 3-back tasks but not at all in the SCD group. These FDR-corrected partial correlations were performed with age, gender and education as covariates.

challenge, M and the N-back task-evoked $CMRO_2$ might have been overestimated in both SCD and control subjects. Although such uncertainties are not likely to alter the differences found between the two groups, they can be avoided with a gas-free approach[68] in future studies. Moreover, the relative results of this study should be validated by means of absolute $CMRO_2$ measurements. Quantitative susceptibility mapping (QSM)-based techniques allow whole-brain absolute $CMRO_2$ measurement without gas manipulation.[69–72] While QSM has the potential to provide neuroimaging biomarkers in various neurodegenerative disorders,[73] few studies have applied it to dynamically measure absolute $CMRO_2$ changes during cognitive tasks, likely due to the relatively lengthy scan time. Recently, our group developed a gas-free MRI technique to dynamically measure the whole-brain oxygen extraction fraction with improved temporal resolution.[74] In the framework of Fick's principle, we intend to combine this technique with CBF measurements to further investigate the absolute changes in whole-brain $CMRO_2$ during cognitive tasks in SCD cohorts.

A second finding of this study was that the impaired cerebral vascular and metabolic responses in SCD were modulated by cognitive processing loads. Despite their normal performance on standardized tests, SCD subjects were reported to slightly underperform in comprehensive cognitive tasks,[13,20–22] a finding that still requires neuroimaging support. The parametric N-back task offers a range of working memory loads and can evoke load-dependent brain activation.[75,76] Load-dependent bilateral frontal hypoactivation during the N-back task has previously been reported in MCI patients.[58] We observed that in the frontal lobe, the differences between the SCD and control groups in all neuroimaging parameters became significant during the most challenging 3-back task despite indistinguishable task performance. Dumas et al.[11] observed that cognitive complainers had increased BOLD activation in relevant brain regions for the 2- and 3-back conditions but equivalent BOLD activation for the 1-back condition compared with the noncomplainers. Erk et al.[8] reported that no difference was found in 2-back-evoked BOLD activation between groups of subjects with and without subjective memory impairment. Considering the differences among individuals and sensitivities of neuroimaging parameters, our study and previous studies jointly supported the concept that sufficiently complex tasks increase the probability of differentiating the SCD group from the control group.

Of the neuroimaging parameters measured and evaluated in this study, δCBF and $\delta CMRO_2$ in the frontal lobe not only had the closest relationships with global cognitive status (Figure 5) but also showed the greatest flexibility in detecting altered N-back task-evoked responses in SCD. In the control group, the frontal δCBF and $\delta CMRO_2$ increased with task difficulty, as previously demonstrated.[11,75] In the SCD group, these parameters behaved in the same manner during the 1- and 2-back tasks but did not further increase during the 3-back task (Figure 3). These observations suggested that the blood flow and metabolic regulation systems in the frontal regions of the SCD group may have been slightly disrupted to an extent that, while still functioning properly during easy to moderate tasks, it was likely to reach its limit during challenging tasks. Therefore, our findings suggest the possibility of a task-load-dependent approach to SCD assessment using CBF and $CMRO_2$ as potential neuroimaging markers.

This study has limitations. For example, the simultaneous acquisition technique provided limited spatial coverage. However, regional heterogeneity in the task-related responses of SCD subjects has been reported in this and previous studies.[8] We chose to observe parts of the frontal and parietal lobes that are known to participate in the working memory process. Nevertheless, task-related responses in other important regions, such as the hippocampus and medial temporal lobe, are not known. In addition, although efforts were made to maintain consistency among subjects by determining the targeted imaging slice using a functional localizing run, it could not be guaranteed that the exact same regions were covered in every subject. As a result, coregistration or voxelwise comparison between groups could not be rigorously conducted, which may blur possible spatial variations in the observed regions. Finally, this cross-sectional study recruited a relatively small sample of elderly individuals without testing for the presence of AD-related pathophysiological biomarkers. SCD is a heterogeneous condition with multiple etiologies,[1] which may hinder a clear understanding of the pathophysiology of AD. To include SCD subjects with an increased risk for cognitive decline, we selected those with memory complaints and associated concerns that had emerged within the past 5 years according to the framework proposed by Jessen et al.[1,2] We obtained statistically significant preliminary evidence demonstrating impaired cerebral vascular and metabolic responses in SCD subjects during cognitive tasks. Nevertheless, longitudinal studies with a large sample size are required to further associate the findings of this study with the risk of AD in the long term.

Funding

The author(s) disclosed receipt of the following financial support for the research, authorship, and/or publication of this article: This work was supported by the National Natural Science Foundation of China (81790650, 81790651, 81727808, 31421003, 61633018, 81601484 and 81901722); Interdisciplinary Program of Shanghai Jiao Tong University (YG2021QN40, 21X010500734); Guangdong key basic research grant (2018B030332001); Guangdong Pearl River Talents Plan (2016ZT06S220) and National Key Research and Development Program of China (2018YFC1312001).

Acknowledgements

The authors thank the National Center for Protein Sciences at Peking University in Beijing, China, for assistance with MRI data acquisition and analysis.

Declaration of conflicting interests

The author(s) declared no potential conflicts of interest with respect to the research, authorship, and/or publication of this article.

Authors' contributions

JG, YH and HL conceived and designed the study. YZ, WD, Y Yin, ZL and Y Yang recruited subjects and participated in data acquisition and analysis. YZ, WD, JG and YH interpreted the results and drafted the manuscript. All authors critically revised and approved the manuscript.

References

1. Jessen F, Amariglio RE, Buckley RF, et al. The characterisation of subjective cognitive decline. *Lancet Neurol* 2020; 19: 271–278.
2. Jessen F, Amariglio RE, van Boxtel M, et al. A conceptual framework for research on subjective cognitive decline in preclinical Alzheimer's disease. *Alzheimers Dement* 2014; 10: 844–852.
3. Jessen F, Wiese B, Bachmann C, et al. Prediction of dementia by subjective memory impairment: effects of severity and temporal association with cognitive impairment. *Arch Gen Psychiatry* 2010; 67: 414–422.
4. van Harten AC, Mielke MM, Swenson-Dravis DM, et al. Subjective cognitive decline and risk of MCI: the Mayo clinic study of aging. *Neurology* 2018; 91: e300–e312.
5. Mitchell AJ, Beaumont H, Ferguson D, et al. Risk of dementia and mild cognitive impairment in older people with subjective memory complaints: meta-analysis. *Acta Psychiatr Scand* 2014; 130: 439–451.
6. Viviano RP and Damoiseaux JS. Functional neuroimaging in subjective cognitive decline: current status and a research path forward. *Alzheimers Res Ther* 2020; 12: 23.
7. Jones DT, Knopman DS, Gunter JL, et al. Cascading network failure across the Alzheimer's disease spectrum. *Brain* 2016; 139: 547–562.
8. Erk S, Spottke A, Meisen A, et al. Evidence of neuronal compensation during episodic memory in subjective

memory impairment. *Arch Gen Psychiatry* 2011; 68: 845–852.
9. Rodda J, Dannhauser T, Cutinha DJ, et al. Subjective cognitive impairment: functional MRI during a divided attention task. *Eur Psychiatry* 2011; 26: 457–462.
10. Rodda JE, Dannhauser TM, Cutinha DJ, et al. Subjective cognitive impairment: increased prefrontal cortex activation compared to controls during an encoding task. *Int J Geriatr Psychiatry* 2009; 24: 865–874.
11. Dumas JA, Kutz AM, McDonald BC, et al. Increased working memory-related brain activity in middle-aged women with cognitive complaints. *Neurobiol Aging* 2013; 34: 1145–1147.
12. Hayes JM, Tang L, Viviano RP, et al. Subjective memory complaints are associated with brain activation supporting successful memory encoding. *Neurobiol Aging* 2017; 60: 71–80.
13. Hu X, Uhle F, Fliessbach K, et al. Reduced future-oriented decision making in individuals with subjective cognitive decline: a functional MRI study. *Alzheimers Dement (Amst)* 2017; 6: 222–231.
14. Park DC and Reuter-Lorenz P. The adaptive brain: aging and neurocognitive scaffolding. *Annu Rev Psychol* 2009; 60: 173–196.
15. Sun Y, Dai Z, Li Y, et al. Subjective cognitive decline: mapping functional and structural brain changes – a combined resting-state functional and structural MR imaging study. *Radiology* 2016; 281: 185–192.
16. Hays CC, Zlatar ZZ, Campbell L, et al. Subjective cognitive decline modifies the relationship between cerebral blood flow and memory function in cognitively normal older adults. *J Int Neuropsychol Soc* 2018; 24: 213–223.
17. Scheef L, Spottke A, Daerr M, et al. Glucose metabolism, gray matter structure, and memory decline in subjective memory impairment. *Neurology* 2012; 79: 1332–1339.
18. Shu N, Wang X, Bi Q, et al. Disrupted topologic efficiency of white matter structural connectome in individuals with subjective cognitive decline. *Radiology* 2018; 286: 229–238.
19. Ogawa S, Menon RS, Tank DW, et al. Functional brain mapping by blood oxygenation level-dependent contrast magnetic resonance imaging. A comparison of signal characteristics with a biophysical model. *Biophys J* 1993; 64: 803–812.
20. Koppara A, Frommann I, Polcher A, et al. Feature binding deficits in subjective cognitive decline and in mild cognitive impairment. *J Alzheimers Dis* 2015; 48: S161–S170.
21. Smart CM and Krawitz A. The impact of subjective cognitive decline on Iowa gambling task performance. *Neuropsychology* 2015; 29: 971–987.
22. Hsu YH, Huang CF, Tu MC, et al. Prospective memory in subjective cognitive decline: a preliminary study on the role of early cognitive marker in dementia. *Alzheimer Dis Assoc Disord* 2015; 29: 229–235.
23. Yang Y, Gu H and Stein EA. Simultaneous MRI acquisition of blood volume, blood flow, and blood oxygenation information during brain activation. *Magn Reson Med* 2004; 52: 1407–1417.
24. Zhang Y, Yin Y, Li H, et al. Measurement of CMRO2 and its relationship with CBF in hypoxia with an extended calibrated BOLD method. *J Cereb Blood Flow Metab* 2020; 40: 2066–2080.
25. Lin AL, Fox PT, Yang Y, et al. Time-dependent correlation of cerebral blood flow with oxygen metabolism in activated human visual cortex as measured by fMRI. *Neuroimage* 2009; 44: 16–22.
26. Lin AL, Fox PT, Hardies J, et al. Nonlinear coupling between cerebral blood flow, oxygen consumption, and ATP production in human visual cortex. *Proc Natl Acad Sci U S A* 2010; 107: 8446–8451.
27. Lin AL, Fox PT, Yang Y, et al. Evaluation of MRI models in the measurement of CMRO2 and its relationship with CBF. *Magn Reson Med* 2008; 60: 380–389.
28. Gu H, Stein EA and Yang Y. Nonlinear responses of cerebral blood volume, blood flow and blood oxygenation signals during visual stimulation. *Magn Reson Imaging* 2005; 23: 921–928.
29. Glielmi CB, Schuchard RA and Hu XP. Estimating cerebral blood volume with expanded vascular space occupancy slice coverage. *Magn Reson Med* 2009; 61: 1193–1200.
30. Goense J, Merkle H and Logothetis NK. High-resolution fMRI reveals laminar differences in neurovascular coupling between positive and negative BOLD responses. *Neuron* 2012; 76: 629–639.
31. Bondi MW, Edmonds EC, Jak AJ, et al. Neuropsychological criteria for mild cognitive impairment improves diagnostic precision, biomarker associations, and progression rates. *J Alzheimers Dis* 2014; 42: 275–289.
32. McKhann GM, Knopman DS, Chertkow H, et al. The diagnosis of dementia due to Alzheimer's disease: recommendations from the national institute on Aging-Alzheimer's association workgroups on diagnostic guidelines for Alzheimer's disease. *Alzheimers Dement* 2011; 7: 263–269.
33. Li X, Wang X, Su L, et al. Sino longitudinal study on cognitive decline (SILCODE): protocol for a Chinese longitudinal observational study to develop risk prediction models of conversion to mild cognitive impairment in individuals with subjective cognitive decline. *BMJ Open* 2019; 9: e028188.
34. Davis TL, Kwong KK, Weisskoff RM, et al. Calibrated functional MRI: mapping the dynamics of oxidative metabolism. *Proc Natl Acad Sci U S A* 1998; 95: 1834–1839.
35. Cheng X, Berman AJL, Polimeni JR, et al. Dependence of the MR signal on the magnetic susceptibility of blood studied with models based on real microvascular networks. *Magn Reson Med* 2019; 81: 3865–3874.
36. Griffeth VE and Buxton RB. A theoretical framework for estimating cerebral oxygen metabolism changes using the calibrated-BOLD method: modeling the effects of blood volume distribution, hematocrit, oxygen extraction fraction, and tissue signal properties on the BOLD signal. *Neuroimage* 2011; 58: 198–212.

37. Shu CY, Sanganahalli BG, Coman D, et al. Quantitative beta mapping for calibrated fMRI. *Neuroimage* 2016; 126: 219–228.
38. Hoge RD, Atkinson J, Gill B, et al. Linear coupling between cerebral blood flow and oxygen consumption in activated human cortex. *Proc Natl Acad Sci U S A* 1999; 96: 9403–9408.
39. Bokde AL, Karmann M, Born C, et al. Altered brain activation during a verbal working memory task in subjects with amnestic mild cognitive impairment. *J Alzheimers Dis* 2010; 21: 103–118.
40. Yetkin FZ, Rosenberg RN, Weiner MF, et al. FMRI of working memory in patients with mild cognitive impairment and probable Alzheimer's disease. *Eur Radiol* 2006; 16: 193–206.
41. Melrose RJ, Jimenez AM, Riskin-Jones H, et al. Alterations to task positive and task negative networks during executive functioning in mild cognitive impairment. *Neuroimage Clin* 2018; 19: 970–981.
42. Alichniewicz KK, Brunner F, Klunemann HH, et al. Structural and functional neural correlates of visuospatial information processing in normal aging and amnestic mild cognitive impairment. *Neurobiol Aging* 2012; 33: 2782–2797.
43. Sweeney MD, Montagne A, Sagare AP, et al. Vascular dysfunction-The disregarded partner of Alzheimer's disease. *Alzheimers Dement* 2019; 15: 158–167.
44. Sweeney MD, Kisler K, Montagne A, et al. The role of brain vasculature in neurodegenerative disorders. *Nat Neurosci* 2018; 21: 1318–1331.
45. Kisler K, Nelson AR, Montagne A, et al. Cerebral blood flow regulation and neurovascular dysfunction in Alzheimer disease. *Nat Rev Neurosci* 2017; 18: 419–434.
46. Chen JJ. Functional MRI of brain physiology in aging and neurodegenerative diseases. *Neuroimage* 2019; 187: 209–225.
47. Leeuwis AE, Benedictus MR, Kuijer JPA, et al. Lower cerebral blood flow is associated with impairment in multiple cognitive domains in Alzheimer's disease. *Alzheimers Dement* 2017; 13: 531–540.
48. Xekardaki A, Rodriguez C, Montandon ML, et al. Arterial spin labeling may contribute to the prediction of cognitive deterioration in healthy elderly individuals. *Radiology* 2015; 274: 490–499.
49. Wang J, Aguirre GK, Kimberg DY, et al. Arterial spin labeling perfusion fMRI with very low task frequency. *Magn Reson Med* 2003; 49: 796–802.
50. Gauthier CJ, Madjar C, Desjardins-Crepeau L, et al. Age dependence of hemodynamic response characteristics in human functional magnetic resonance imaging. *Neurobiol Aging* 2013; 34: 1469–1485.
51. Xu G, Antuono PG, Jones J, et al. Perfusion fMRI detects deficits in regional CBF during memory-encoding tasks in MCI subjects. *Neurology* 2007; 69: 1650–1656.
52. Xie L, Dolui S, Das SR, et al. A brain stress test: cerebral perfusion during memory encoding in mild cognitive impairment. *Neuroimage Clin* 2016; 11: 388–397.
53. Lu H, Hua J and van Zijl PC. Noninvasive functional imaging of cerebral blood volume with vascular-space-occupancy (VASO) MRI. *NMR Biomed* 2013; 26: 932–948.
54. Grubb RL Jr, Raichle ME, Eichling JO, et al. The effects of changes in PaCO2 on cerebral blood volume, blood flow, and vascular mean transit time. *Stroke* 1974; 5: 630–639.
55. Xu G, Wu G, Xu Y, et al. Decrease in $CMRO_2$ for memory-encoding tasks in the hippocampus of mild cognitive impairment subjects. In: *Proceedings of the 14th International Society for Magnetic Resonance in Medicine Scientific Meeting*, Seattle, WA, 6–12 May 2006, p.1108. California (CA): ISMRM.
56. Tak S, Yoon SJ, Jang J, et al. Quantitative analysis of hemodynamic and metabolic changes in subcortical vascular dementia using simultaneous near-infrared spectroscopy and fMRI measurements. *Neuroimage* 2011; 55: 176–184.
57. Tak S, Jang J, Lee K, et al. Quantification of CMRO(2) without hypercapnia using simultaneous near-infrared spectroscopy and fMRI measurements. *Phys Med Biol* 2010; 55: 3249–3269.
58. Yeung MK, Sze SL, Woo J, et al. Reduced frontal activations at high working memory load in mild cognitive impairment: near-infrared spectroscopy. *Dement Geriatr Cogn Disord* 2016; 42: 278–296.
59. Niu H, Zhu Z, Wang M, et al. Abnormal dynamic functional connectivity and brain states in Alzheimer's diseases: functional near-infrared spectroscopy study. *Neurophotonics* 2019; 6: 025010.
60. Vermeij A, Kessels RPC, Heskamp L, et al. Prefrontal activation may predict working-memory training gain in normal aging and mild cognitive impairment. *Brain Imaging Behav* 2017; 11: 141–154.
61. Yeung MK and Chan AS. Functional near-infrared spectroscopy reveals decreased resting oxygenation levels and task-related oxygenation changes in mild cognitive impairment and dementia: a systematic review. *J Psychiatr Res* 2020; 124: 58–76.
62. Vannini P, Hanseeuw B, Munro CE, et al. Hippocampal hypometabolism in older adults with memory complaints and increased amyloid burden. *Neurology* 2017; 88: 1759–1767.
63. Risacher SL, Kim S, Nho K, et al. APOE effect on Alzheimer's disease biomarkers in older adults with significant memory concern. *Alzheimers Dement* 2015; 11: 1417–1429.
64. Fox PT, Raichle ME, Mintun MA, et al. Nonoxidative glucose consumption during focal physiologic neural activity. *Science* 1988; 241: 462–464.
65. Liu J, Zhu YS, Khan MA, et al. Global brain hypoperfusion and oxygenation in amnestic mild cognitive impairment. *Alzheimers Dement* 2014; 10: 162–170.
66. Sokoloff L, Reivich M, Kennedy C, et al. The [14C]deoxyglucose method for the measurement of local cerebral glucose utilization: theory, procedure, and normal values

in the conscious and anesthetized albino rat. *J Neurochem* 1977; 28: 897–916.
67. Bright MG, Croal PL, Blockley NP, et al. Multiparametric measurement of cerebral physiology using calibrated fMRI. *Neuroimage* 2019; 187: 128–144.
68. Blockley NP, Griffeth VE, Simon AB, et al. Calibrating the BOLD response without administering gases: comparison of hypercapnia calibration with calibration using an asymmetric spin echo. *Neuroimage* 2015; 104: 423–429.
69. Zhang J, Liu T, Gupta A, et al. Quantitative mapping of cerebral metabolic rate of oxygen ($CMRO_2$) using quantitative susceptibility mapping (QSM). *Magn Reson Med* 2015; 74: 945–952.
70. Zhang J, Zhou D, Nguyen TD, et al. Cerebral metabolic rate of oxygen ($CMRO_2$) mapping with hyperventilation challenge using quantitative susceptibility mapping (QSM). *Magn Reson Med* 2017; 77: 1762–1773.
71. Cho J, Kee Y, Spincemaille P, et al. Cerebral metabolic rate of oxygen ($CMRO_2$) mapping by combining quantitative susceptibility mapping (QSM) and quantitative blood oxygenation level-dependent imaging (qBOLD). *Magn Reson Med* 2018; 80: 1595–1604.
72. Zhang J, Cho J, Zhou D, et al. Quantitative susceptibility mapping-based cerebral metabolic rate of oxygen mapping with minimum local variance. *Magn Reson Med* 2018; 79: 172–179.
73. Vinayagamani S, Sheelakumari R, Sabarish S, et al. Quantitative susceptibility mapping: technical considerations and clinical applications in neuroimaging. *J Magn Reson Imaging* 2021; 53: 23–37.
74. Yin Y, Zhang Y and Gao JH. Dynamic measurement of oxygen extraction fraction using a multiecho asymmetric spin echo (MASE) pulse sequence. *Magn Reson Med* 2018; 80: 1118–1124.
75. Zou Q, Gu H, Wang DJ, et al. Quantification of load dependent brain activity in parametric N-back working memory tasks using pseudo-continuous arterial spin labeling (pCASL) perfusion imaging. *J Cogn Sci* 2011; 12: 129–149.
76. Cohen JD, Perlstein WM, Braver TS, et al. Temporal dynamics of brain activation during a working memory task. *Nature* 1997; 386: 604–608.